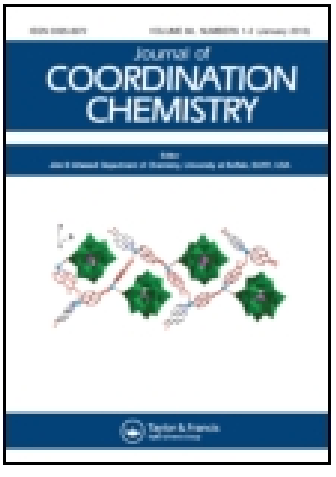

Journal of Coordination Chemistry
Publication details, including instructions for authors and subscription information:
http://www.tandfonline.com/loi/gcoo20

A porous Cu(II)-MOF containing $[PW_{12}O_{40}]^{3-}$ and a large protonated water cluster: synthesis, structure, and proton conductivity

Meilin Wei[a], Lin Chen[a] & Xianying Duan[b]
[a] School of Chemistry and Chemical Engineering, Henan Normal University, Xinxiang, PR China
[b] Institute of Chemistry, Henan Academy of Sciences, Zhengzhou, PR China

Accepted author version posted online: 03 Sep 2014.Published online: 12 Sep 2014.

To cite this article: Meilin Wei, Lin Chen & Xianying Duan (2014) A porous Cu(II)-MOF containing $[PW_{12}O_{40}]^{3-}$ and a large protonated water cluster: synthesis, structure, and proton conductivity, Journal of Coordination Chemistry, 67:17, 2809-2819, DOI: 10.1080/00958972.2014.957689

To link to this article: http://dx.doi.org/10.1080/00958972.2014.957689

Journal of Coordination Chemistry, 2014
Vol. 67, No. 17, 2809–2819, http://dx.doi.org/10.1080/00958972.2014.957689

A porous Cu(II)-MOF containing $[PW_{12}O_{40}]^{3-}$ and a large protonated water cluster: synthesis, structure, and proton conductivity

MEILIN WEI*†, LIN CHEN† and XIANYING DUAN‡

†School of Chemistry and Chemical Engineering, Henan Normal University, Xinxiang, PR China
‡Institute of Chemistry, Henan Academy of Sciences, Zhengzhou, PR China

(*Received 2 March 2014; accepted 15 July 2014*)

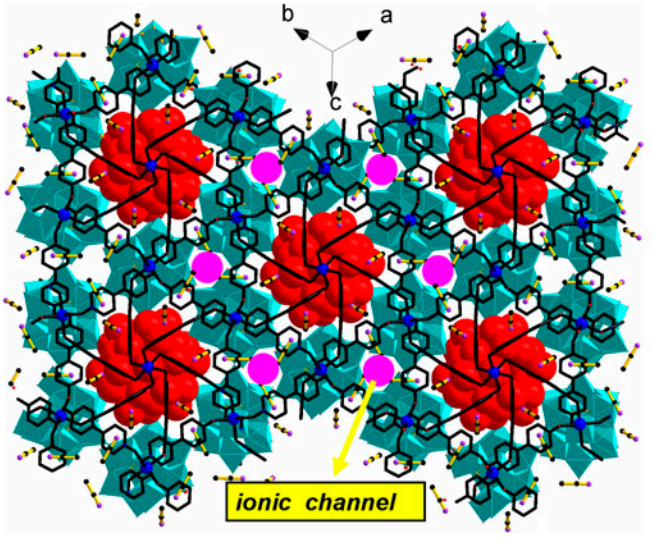

A proton-conducting metal–organic framework (MOF), $\{[Cu_4(dpdo)_{12}][H(H_2O)_{27}(CH_3CN)_{12}][PW_{12}O_{40}]_3\}_n$ (where dpdo is 4,4′-bipyridine-*N*,*N*′-dioxide) (**1**), was synthesized by the reaction of $CuHPW_{12}O_{40}{\cdot}nH_2O$ and dpdo at room temperature. Single-crystal X-ray diffraction analysis at 293 K revealed that **1** crystallized in the cubic space group *I*m-3 and presented a non-interwoven 3-D framework with cubic cavities and guest molecules. A large ionic water cluster $H^+(H_2O)_{27}$, consisting of a water shell $(H_2O)_{26}$ and an encaged $H^+(H_2O)$ as a center core, was trapped in the cubic cavity of the MOF $\{[Cu_4(dpdo)_{12}(PW_{12}O_{40})_3]^-\}_\infty$. Thermogravimetric analysis suggests that **1** has high thermal stability, indicating that such a non-interwoven 3-D framework with cubic cavities is a suitable host for researching protonated water clusters. Its water vapor adsorption isotherm at room temperature and pressure shows that the water vapor adsorbed in it was 65.1 $cm^3\,g^{-1}$ at the maximum allowable humidity. It exhibits good proton conductivities of 10^{-5}–$10^{-4}\,S\,cm^{-1}$ at 100 °C in the relative humidity range 35–98%.

*Corresponding author. Email: weimeilin@henannu.edu.cn

Keywords: Polyoxometalates; Crystal structure; Metal–organic framework; 4,4′-Bipyridine-*N*,*N*′-dioxide; Proton conductivity

1. Introduction

Proton conductivity in solid-state materials has interest for transport dynamics and its applications in fuel cells [1–4]. Proton conductivity is strongly influenced by the microstructure of the conductors. Ordered MOF structures provide valuable anchor points for establishing structure–activity relationships in proton-conducting solids, essentially a firm handhold for modeling [3, 4]. We have been interested in encapsulating large-sized proton-hydrated species by synthetic receptors as MOFs [5]. The lattice of a predesigned crystal host can provide an attractive environment to stabilize protonated water clusters with special structures, and then the relevant crystallographic characterization could offer detailed structural information, which cannot be directly obtained with other experimental methods. So far, we explored simple building blocks, 4,4′-bipyridine-*N*,*N*′-dioxide (dpdo) and Co^{2+} (or Ni^{2+}) ions, for the syntheses of three compounds, $\{[Co_4(dpdo)_{12}][H(H_2O)_{27}(CH_3CN)_{12}][PW_{12}O_{40}]_3\}_n$, $\{[Co_4(dpdo)_{12}][H(H_2O)_{28}(CH_3CN)_{12}][PMo_{12}O_{40}]_3\}_n$ and $\{[Ni_4(dpdo)_{12}][H(H_2O)_{27}(CH_3CN)_{12}][PW_{12}O_{40}]_3\}_n$, with the aid of large $[PW_{12}O_{40}]^{3-}$ and $[PMo_{12}O_{40}]^{3-}$ anions as the templates and pillars. Each compound has a 3-D porous metal–organic framework (MOF) with cubic symmetries, $\{[Co_4(dpdo)_{12}][(CH_3CN)_{12}][PW_{12}O_{40}]_3\}_n$, $\{[Co_4(dpdo)_{12}][(CH_3CN)_{12}][PMo_{12}O_{40}]_3\}_n$, and $\{[Ni_4(dpdo)_{12}][(CH_3CN)_{12}][PW_{12}O_{40}]_3\}_n$. In these MOFs, as crystal hosts, two large-sized protonated water clusters $H^+(H_2O)_{27}$ and $H^+(H_2O)_{28}$ with clathrate structures, in which an unattached hydronium core ion (H_3O^+) or a $H^+(H_2O)_2$ core ion is surrounded by a water shell $(H_2O)_{26}$ and is located at the crystallographic center of the host, have been encapsulated [5]. It is important to explore new MOFs as crystal hosts of protonated water clusters with special structures. Now, we use simple building blocks (dpdo, $[PW_{12}O_{40}]^{3-}$, Cu^{2+}, and imidazole molecules) to synthesize a new compound, $\{[Cu_4(dpdo)_{12}][H(H_2O)_{27}(CH_3CN)_{12}][PW_{12}O_{40}]_3\}_n$ (**1**). Compound **1** also has a 3-D porous MOF with cubic symmetry, $\{[Cu_4(dpdo)_{12}][(CH_3CN)_{12}][PW_{12}O_{40}]_3\}_n$. In **1**, the $H^+(H_2O)_{27}$ with clathrate structure, in which an unattached hydronium core ion (H_3O^+) is surrounded by a water shell $(H_2O)_{26}$ and is located at the crystallographic center of the host, has been encapsulated. Compound **1** is interesting for constructing a proton conductor because it has crystalline structure. Detailed structural analysis of **1** indicates that it has a key structural basis of proton or ion conductivity in solid-state materials, i.e. proton carriers (such as H_3O^+ or H^+) and proton-conducting pathways. Compound **1** shows proton conductivities across a wide range of temperatures and relative humidity (RH) and achieves a proton conductivity over 10^{-4} S cm^{-1} at 100 °C under 98% RH. Here, we report its synthesis, crystal structure, and proton conductivity.

2. Experimental

2.1. *Materials and measurements*

All organic solvents and materials used for synthesis were of reagent grade and used without purification. α-$H_3PW_{12}O_{40}\cdot 6H_2O$ was prepared according to a literature method [2, 3]

and characterized by IR spectra and TG analyses. Elemental analyses (C, H, and N) were carried out on a Perkin Elmer 240C analyzer. X-ray powder diffraction was performed on a Bruker D8 Avance Instrument using Cu-Kα radiation and a fixed power source (40 kv, 40 mA). IR spectra were recorded on a VECTOR 22 Bruker spectrophotometer with KBr pellets from 400 to 4000 cm^{-1} at room temperature. Thermogravimetric analysis was performed on a Perkin Elmer thermal analyzer under nitrogen at a heating rate of 10 °C min^{-1}. Water absorption experiments were performed on an AQUAL-ABVSA. For an electrical conductivity study, the powdered crystalline samples were compressed to 0.8–1.0 mm in thickness and 12.0 mm in diameter under a pressure of 12–14 MPa. AC impedance spectroscopy measurement was performed on a chi660d (Shanghai chenhua) electrochemical impedance analyzer with copper electrodes [2, 3] (the purity of Cu is more than 99.8%) over the frequency range from 10^5 to 10 Hz. Samples were placed in a temperature–humidity controlled chamber (GT-TH-64Z, Dongwan Gaotian Corp.) The conductivity was calculated as $\sigma = (1/R) \times (h/S)$, where R is the resistance, h is the thickness, and S is the area of the tablet.

2.2. *Synthesis of $\{[Cu(dpdo)_3]_4[H(H_2O)_{27}(CH_3CN)_{12}](PW_{12}O_{40})_3\}_n$ (1)*

The copper salt ($CuHPW_{12}O_{40}\cdot nH_2O$) was prepared by mixing α-$H_3PW_{12}O_{40}\cdot 6H_2O$ (84 mg, 0.04 mM) and $CuCl_2\cdot 6H_2O$ (10 mg, 0.04 mM) in water (1.5 mL), and then drying the solution at 80 °C in a water bath. A buffer layer of a solution (10 mL) of acetonitrile/water (3 : 2, v/v) was carefully layered over an aqueous solution of 4,4′-bipyridine-*N,N′*-dioxide hydrate (33 mg, 0.15 mM) and imidazole (about 2.8 mg, 0.04 mM). Then a solution of $CuHPW_{12}O_{40}\cdot nH_2O$ in acetonitrile/water mixture (3 : 1, v/v) (4 mL) was carefully layered over the buffer layer. Red block single crystals appeared after 4–5 weeks. Yield: 64 mg, 76% based on polyoxometalates. Anal. Calcd (%) for $C_{144}H_{187}N_{36}O_{171}Cu_4W_{36}P_3$ (%): C, 14.26; H, 1.55; N, 4.16. Found (%): C, 14.18; H, 1.49; N, 4.08. IR (KBr) ν, cm^{-1}: 803 $\nu(W–O_c)$, 896 $\nu(W–O_b)$, 977 $\nu(W–O_t)$, 1078 $\nu(P–O_a)$ (four characteristic vibrations of heteropolyanions with Keggin structure; O_t refers to terminal oxygen atoms connecting one W atom, O_b refers to atoms located in a shared corner between two W_3O_{13} units, and O_c refers to oxygen atoms connecting edge-sharing WO_6 octahedra in a W_3O_{13} unit); ν(N–O) (1224 cm^{-1}), ν (ring) (1475 cm^{-1}), δ (C–H, in plane) (1180 cm^{-1}), and δ(N–O) (840 cm^{-1}) (four characteristic vibrations resulting from dpdo molecules). Compound **1** was simply synthesized by the reaction of $CuHPW_{12}O_{40}\cdot nH_2O$, dpdo, and imidazole at room temperature. However, **1** could not be obtained through the reaction of $CuHPM_{12}O_{40}\cdot nH_2O$ and dpdo. Although imidazole was used as a starting material in the reaction and was indispensable for the preparation of **1**, there was no imidazole in **1**. The specific role of defined amounts of imidazole in the synthesis of **1** is not well understood, and imidazole may play a synergistic action with other components in the reactions. Similar cases were reported [3].

2.3. *Crystal structure and determination*

Intensity data of **1** were collected on a Siemens SMART-CCD diffractometer with graphite-monochromated Mo-Kα radiation (λ = 0.71073) using SMART and SAINT [6]. The structure was solved by direct methods and refined on F^2 using full-matrix least-squares with SHELXTL version 5.1 [7]. Non-hydrogen atoms were refined anisotropically, except for the disordered oxygens. Hydrogens of organic molecules were localized in their calculated

Table 1. Crystallographic data and refinement parameters for **1**.

Empirical formula	$C_{144}H_{187}N_{36}O_{171}Cu_4W_{36}P_3$
Mr	12123.97
Crystal system	Cubic
Space group	Im-3
a (Å)	23.1885(2)
V (Å^3)	12468.61(19)
Z	2
D_{Calcd} (g cm^{-3})	3.229
μ (mm^{-1})	16.996
F (000)	10,992
Refl. measured	17,405
Refl. unique	1814
R_{int}	0.1017
Refinement parameters	171
GOF on F^2	1.095
R_1/wR_2 [$I \geq 2\sigma(I)$]	0.0629/0.1392
R_1/wR_2 (all data)	0.0742/0.1438
$\Delta\rho_{(max)}$ and $\Delta\rho_{(min)}$, e Å^{-3}	2.548 and −2.012

positions and refined using a riding model. Hydrogens of water molecules were not treated. The oxygens of the P–O groups were disordered into two positions with the site occupancy factor (SOF) fixed at 0.25. The water molecules of the type O(3W) positioned in each face of the $(H_2O)_{20}$ hexahedron were disordered with the SOF fixed at 0.25. The crystal parameters, data collection, and refinement results are summarized in table 1.

3. Results and discussion

3.1. *Structure description*

Compound **1** was characterized by single-crystal X-ray diffraction, infrared spectroscopy, and thermogravimetric and elemental analyses. X-ray diffraction analysis at 293 K revealed that **1** crystallized in the cubic space group *I*m-3, exhibiting similar unit cell parameters and structural features as porous MOFs based-on Co^{2+} and Ni^{2+} [5].

Compound **1** is composed of a non-interwoven 3-D framework with cubic cavities and guest molecules. As shown in figure 1, each Cu(II) is coordinated by six identical dpdo ligands, forming an ideal octahedral coordination geometry, while each dpdo ligand bridges two identical Cu(II) centers alternatively to form the 3-D framework. Although the Cu···Cu separations in all directions are 11.59 Å, half of an axial length, the windows of the cubic cavities seem to be rectangular since the N(dpdo)–O(dpdo)–Cu(II) angles are not right angles but ca. 120°. The Keggin structure $[PW_{12}O_{40}]^{3-}$ anions, with a diameter of about 10.4 Å, fit the cubic cavities very well, avoiding potential interpenetrations of the framework. Since the template anion $[PW_{12}O_{40}]^{3-}$ is typically trivalent and the corresponding Cu(II)$(dpdo)_3$ unit of a cubic cavity is positive divalent, only some of the cavities would be filled by the anions as charge compensation. As evidenced by X-ray analysis, three quarters of the cavities are occupied by $[PW_{12}O_{40}]^{3-}$ anions and another quarter of the cavities is filled with large water clusters (figure 2). Under the current synthetic and crystallization conditions, the most likely scenario is that the water cluster is protonic to maintain electrical

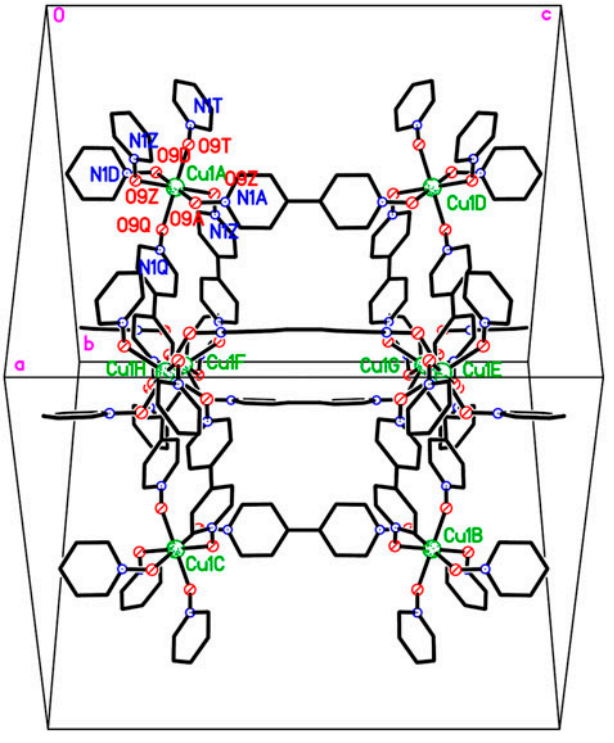

Figure 1. Perspective of the 3-D framework $\{[Cu(dpdo)_3]n\}^{2n+}$ in **1**. Hydrogens are omitted for clarity. Selected bond distance (Å): Cu(1)–O(9) 2.068(8).

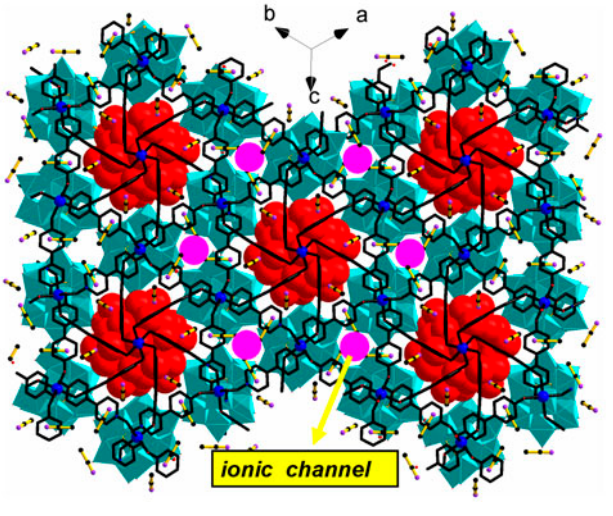

Figure 2. Packing diagrams of **1** viewed along the (1, 1, 1) direction showing the potential ionic channels constrained by the $[PW_{12}O_{40}]^{3-}$ anions and the dpdo ligands as well as the protonated water cluster. The wire/stick diagram represents the robust $[Cu_4(dpdo)_{12}]_\infty$ framework, the polyhedral diagram represents the $[PW_{12}O_{40}]^{3-}$ anion that occupies three-quarters of the cavities, the space-filling diagram represents the possible water cluster that occupies a quarter of the cavities of the MOF, and the purple circle represents the ionic channel, respectively.

neutrality throughout the crystal. Around each water cluster, eight Cu^{2+} ions are situated at the vertices of the cubic cavity and six identical $[PW_{12}O_{40}]^{3-}$ anions sit in six neighboring cavities. These ionic species together form a specific pseudo-spherical static field, which not only is an ideal environment for stabilizing protonic water clusters but also repels the proton toward the center of the water cluster rather than keeping it located on the surface. In addition, there are weak C–H(acetonitrile)···O($[PW_{12}O_{40}]^{3-}$) hydrogen bonds with a C···O separation of 3.235(5) Å between acetonitrile and polyanion and strong O–H(water cluster)···N(acetonitrile) hydrogen bonds with a N···O separation of 2.883(4) Å between the water cluster and acetonitrile molecule. Consequently, these acetonitrile molecules form an amphiphilic global shield layer with their hydrophobic methyl groups pointing toward the outer polyanions and the hydrophilic C≡N ends directing toward the center of the cavity, providing a hydrophilic environment that is beneficial to the molecular recognition and stabilization of specific water clusters.

Each $H^+(H_2O)_{27}$ cluster in the cavity of **1** comprises a $(H_2O)_{26}$ water shell acting as a "sub-host" and an unattached hydronium core ion (H_3O^+) as a "guest" (figure 3). There are three types of water molecules in the $(H_2O)_{26}$ water shells according to the position. Eight water molecules O(2W) and 12 other water molecules O(1W) are linked forming a $(H_2O)_{20}$ hexahedron with each of its faces depicted as an octagonal water ring $(H_2O)_8$. The residual space of the cavity is filled by six additional water molecules O(3W) that embed in the six faces of the $(H_2O)_{20}$ hexahedral shell, respectively.

Detailed structural analysis of **1** indicates that it contains potential channels passing through the framework and surrounded by water clusters and polyanions. As shown in figure 2, each channel is perpendicular to, and passes through, a right triangle defined by three identical anions in a (1, 1, 1) plane, together with a dpdo ligand that compresses the channel down to about 3.3 Å in radius. On this plane, a protonated water cluster sits by the triangle, forming a square with three anions. It is likely that these channels only admit passage of some small species, such as hydronium ions or water molecules [5]. These unique structural features of **1**, i.e. $H^+(H_2O)_{27}$ clusters filled in the high-dielectric conduction pores

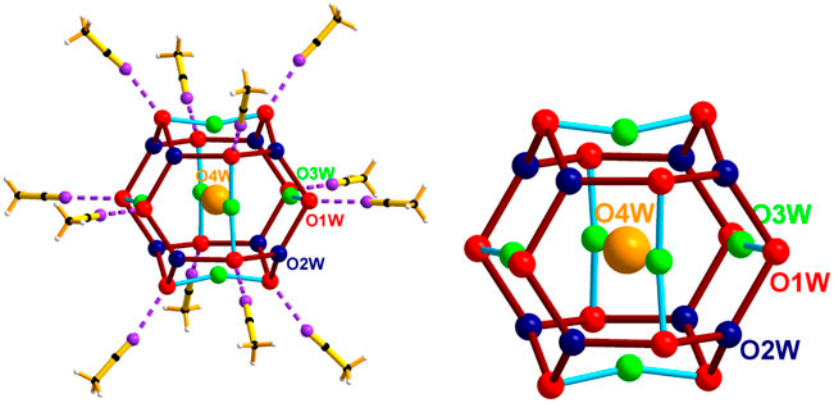

Figure 3. Perspective of the $[H^+(H_2O)_{27}(CH_3CN)_{12}]$ and $[H^+(H_2O)_{27}]$ clusters, showing the $(H_2O)_{26}$ shell formed by the 12 O(1W) (red), eight O(2W) (blue), and six O(3W) (green), and the monowater center O(4W) (orange) as well as the acetonitrile dangling outside with the nitrogen atoms (purple) hydrogen bonding to the O(1 W) centers. Selected atom···atom separations (Å): O(1W)···O(2W) 2.793(4), O(1W)···O(3W) 2.569(5), O(1W)···N(2) 2.883(4) (see http://dx.doi.org/10.1080/00958972.2014.957689 for color version).

with their radii up to about 10 Å and the long channels with their radii of about 3.3 Å, suggest that a key structural basis of proton or ion conductivity in solid-state materials, i.e. proton carriers (such as H_3O^+ or H^+) and proton-conducting pathways, could be achieved in **1**. The robust crystallinity of MOFs not only traps the usually non-isolatable water clusters but also facilitates their X-ray analysis, giving us a great opportunity to explore the proton transfer associated with these finite water clusters. Studies on proton conductivity of **1** were conducted by a complex-plane impedance method. Compound **1** will provide valuable anchor points for establishing the relationships between isolated protonic water clusters with clathrate structure and proton conductivity of MOFs, essentially a firm handhold for modeling.

POMs present a wide range of intriguing topologies and structures, and whose spherical surfaces give an opportunity for forming coordination bonds or hydrogen bonds with organic or inorganic moieties [8]. Representative examples include $(C_7N_2H_7)_3(C_7N_2H_6)\cdot PMo_{12}O_{40}\cdot 2H_2O$ and $(C_7N_2H_7)_3(C_7N_2H_6)_2\cdot AsMo_{12}O_{40}\cdot 3H_2O$ ($C_7N_2H_6$ = benzimidazole) [8i], $[Co(pyim)_3][HPW_{12}O_{40}]\cdot 4H_2O$, and $[Ni(pyim)_3]_2[(PMo_{11}O_{40})$-Mo-V-O-VI$]\cdot 1.5H_2O$ (pyim = 2-(2-pyridyl)-imidazole) [8j], $\{[Zn_3Na_2(OH)_2(bpdo)_6(H_2O)_{16}][PW_{12}O_{40}]_2\}(bpdo)_3\cdot C_2H_5OH\cdot 2H_2O$ (bpdo = 4,4-bis(pyridine-N-oxide)) and $[CuCl(Phen)(H_2O)][PW_{12}O_{40}][4,4'\text{-}H_2bpy]\cdot 1.5H_2O$ [8k], as well as $[Cd_2(Phen)_4Cl_2][HPMo_{12}O_{40}](4,4'\text{-bpy})$ (bpy = bipyridine, Phen = phenanthroline) [8l]. Interestingly, in **1**, $[PW_{12}O_{40}]^{3-}$ anions do not form coordination bonds and hydrogen bonds with organic or inorganic moieties, but fill in the cavities of the MOF as guest molecules. In the $[PW_{12}O_{40}]^{3-}$ units of **1**, the central P atom is surrounded by a cube of eight oxygens with each oxygen site half occupied. These eight oxygens are all crystallographically disordered, and this case can be found in many compounds [2–5, 8]. In **1**, the bond lengths of P–O and W–O are 1.391(17)–1.568(16) and 1.643(17)–2.513(16) Å, respectively. The bond lengths of P–O and W–O in **1** are comparable to those in the 3-D porous polyoxometalates-based organic–inorganic hybrid materials with Keggin anions as guests [5]. In addition, the O–P–O angles are 104.9(12)°–112.6(14)°. All these results indicate that the $[PW_{12}O_{40}]^{3-}$ units have a normal Keggin structure in **1**.

3.2. *Thermogravimetric analysis*

TGA of the powder of the crystalline sample of **1** in atmosphere of N_2 shows a weight loss (7.24%) from 25 to 300 °C, corresponding to 27 water molecules and 12 acetonitrile molecules (Calcd 8.05%) (figure 4). Moreover, a weight loss of about 1% from 25 to 100 °C and an endothermal peak at 120 °C suggest the loss of some water molecules in the water cluster. The framework began to decompose at 300 °C, corresponding to disrupting of the structural skeletons of the cation MOF $[Cu(dpdo)_3]^{2+}$ and the template anion $[PW_{12}O_{40}]^{3-}$. The MOF of **1** could be retained below 300 °C, indicating that such a non-interwoven 3-D framework with cubic cavities is a suitable host for researching protonated water clusters. Water retention in the hybrid maerials at high temperature is a key factor for having fast protonic conduction. All these results also indicate that **1** can potentially be a proton-conducting material.

3.3. *Water vapor adsorption isotherm*

To examine the hydrophilicity and capacity for inclusion of water molecules in **1**, we measured its water vapor adsorption isotherm at room temperature and normal pressure

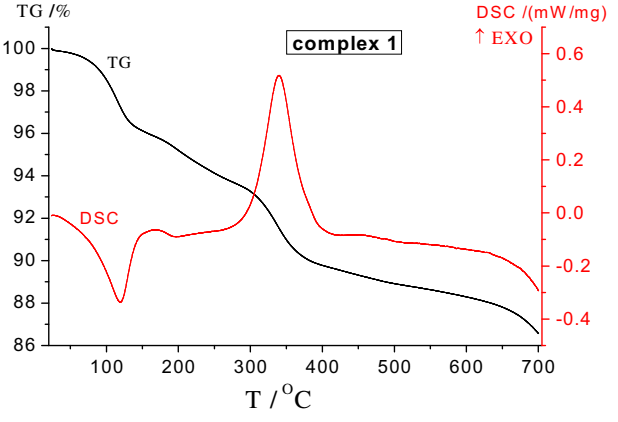

Figure 4. The TG–DSC curves of **1**.

(figure 5). Compound **1** rapidly adsorbs water vapor in the RH range 0–35% and very slowly adsorbs water vapor in the RH range 35–98%. At the maximum allowable humidity, the water vapor adsorbed in **1** was 65.1 $cm^3\ g^{-1}$.

3.4. *Proton conductivity*

The proton conductivity of **1** was measured at 25 °C under 98% RH by a complex-plane impedance method using a compacted pellet of the powdered crystalline sample, which has the same structure as the single crystal (figure 6). At 25 °C, **1** showed poor proton conductivities of $2.71 \times 10^{-7}\ S\ cm^{-1}$ under 98% RH. Again, we measured its ionic conductivities up to 100 °C under 98% RH conditions. As the temperature increases, the proton conductivities of **1** increase on a logarithmic scale even with almost saturated humidities. At

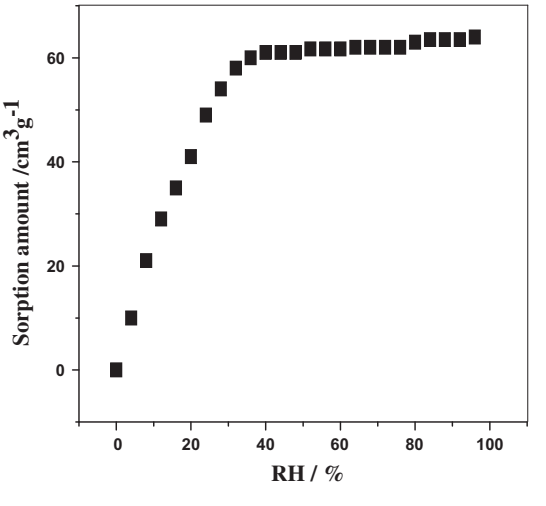

Figure 5. Water vapor absorption isotherms at room temperature and normal pressure.

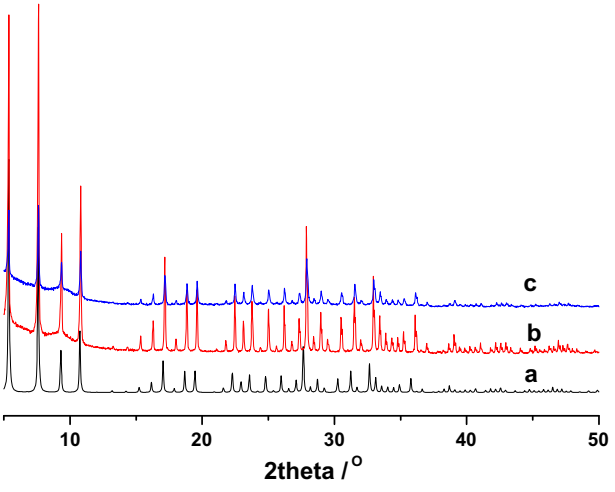

Figure 6. The powder X-ray diffraction data of **1**, the simulated powder pattern (a), the powder before the proton-conductive measurement (b), and the powder after the proton-conductive measurement (c).

100 °C, its proton conductivity reached ~1.25 × 10^{-4} S cm^{-1}. Figure 7 shows the Arrhenius plot of the proton conductivities of **1** from 25 to 100 °C under 98% RH conditions. The lnσT increases almost linearly from 25 to 100 °C and the corresponding activation energy (E_a) of conductivity was estimated to be 0.82 eV. The E_a value is high in the temperature range of 25–100 °C. This is probably due to the fact that protons originating from $H^+(H_2O)_{27}$ clusters need an endothermal process for dissociation as hydrated forms such as H^+, H_3O^+, or other proton species. Therefore, the fact that **1** exhibits good proton conductivities from 85 to 100 °C is indicative of a high carrier concentration based on the dissociating processes of protons from $H^+(H_2O)_{27}$ clusters. The proton conductivities of **1** were also measured at 70 and 100 °C in the RH range 35–98% by a complex-plane impedance method. Figure 8 shows the log σ (S cm^{-1}) *vs.* RH plots of **1** at 70 and 100 °C

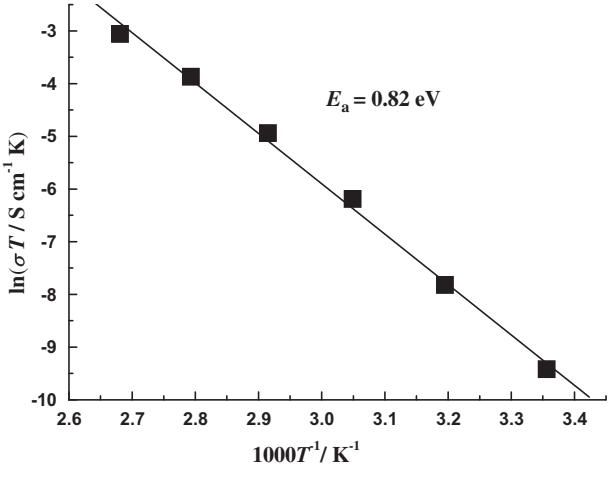

Figure 7. Arrhenius plot of the proton conductivities of **1**.

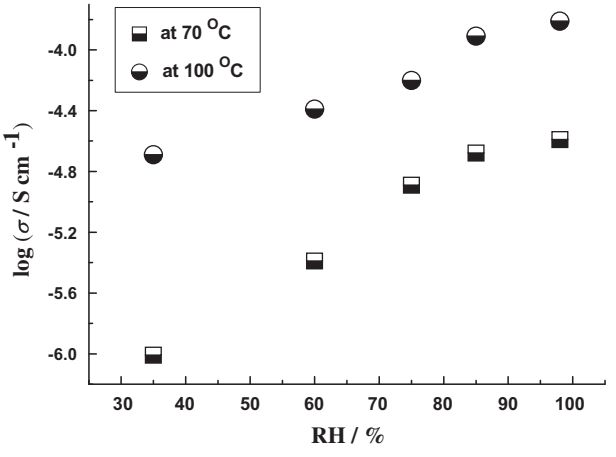

Figure 8. Log σ (S cm^{-1}) *vs.* RH plots of **1** at 70 and 100 °C.

under 35–98% RH. The conductivities of **1** at both temperatures increase with increasing RH. As shown in figure 8, at 35% RH, conductivity of **1** at 100 °C is higher than that at 70 °C. This may be mainly a result of a higher carrier concentration based on the dissociating processes of protons from $H^+(H_2O)_{27}$ clusters. Moreover, there is the possibility of hydrolysis of **1** when it is held at 100 °C with a RH higher than 98% (100%, or condensed water that attack the metal centers). The powder X-ray diffraction data in figure 6 suggested that the powder sample after the proton-conductive measurement has the same framework as that of **1**.

Some work on proton conductivity with PCP (porous coordination polymer)/MOF materials around ambient temperatures under high-humidity conditions have been reported and the composites show a remarkable drop of the conductivity as the temperature increases [9]. Representative examples include $(NH_4)_2(adp)[Zn_2(ox)_3]\cdot 3H_2O$ (adp = adipic acid, ox = oxalate, 8×10^{-3} S cm^{-1} at 25 °C under 98% RH) [9d], $Zn_3(btp)(H_2O)_2\cdot 2H_2O$ (btp = 1,3,5-benzenetriphosphonate, 3.5×10^{-5} S cm^{-1} at 25 °C under 98% RH) [9e], $(Mo_5P_2O_{23})[Cu(phen)(H_2O)]_3\cdot 5H_2O$ (2.2×10^{-5} S cm^{-1} at 28 °C under 98% RH) [9f], and $V[Cr(CN)_6]_{2/3}\cdot 4.2H_2O$ (2.6×10^{-3} S cm^{-1} at 50 °C under 100% RH) [9g]. We also reported proton conductivity with PCP/MOF materials from 25 to 100 °C under 98% RH. Representative examples include $\{H[Cu(Hbpdc)(H_2O)_2]_2[PM_{12}O_{40}]\cdot nH_2O\}_n$ (H_2bpdc = 2,2′-bipyridyl-3,3′-dicarboxylic acid, M = Mo, and W, 10^{-7}–10^{-4} S cm^{-1} at 25 to about 100 °C under 98% RH) [3a], as well as $\{[H(H_2O)_2][Sr(HINO)_4(H_2O)_7(PW_{12}O_{40})]\}_n$ and $\{[H(H_2O)_2][Ca(HINO)_4(H_2O)_5(PW_{12}O_{40})]\}_n$ (HINO = isonicotinic acid N-oxide, 10^{-6}–10^{-3} S cm^{-1} at 25 to about 100 °C under 98% RH) [8h]. The proton conductivity values (10^{-7}–10^{-4} S cm^{-1}) of **1** below 100 °C under 98% RH are comparable to these compounds reported.

In addition, we tested the reproducibility and reversibility of the conductivities of **1** as a function of the temperature and the RH by measuring the proton conduction two to three times on different batches of samples. Each experiment revealed similar results.

As shown in figure 3, the long channels with their radii of about 3.3 Å only admit passage of some small species, such as hydronium ions or water molecules. In addition, the E_a value (0.82 eV) is high. These facts suggest that the mechanism of proton conduction of **1** is similar to that of the vehicle mechanism [10], that is, the direct diffusion of additional protons with water molecules.

4. Conclusion

A proton-conductive MOF with cubic cavities and guest molecules based on $CuHPW_{12}O_{40}{\cdot}nH_2O$ and dpdo molecules has been constructed. A large ionic water cluster $H^+(H_2O)_{27}$ was trapped in the cubic cavity of the MOF, $\{[Cu_4(dpdo)_{12}(PW_{12}O_{40})_3]^-\}_\infty$. Compound **1** exhibits proton conductivities of 10^{-5}–10^{-4} S cm^{-1} at 100 °C in the RH range 35–98%. Compound **1** provides a new route to construct proton-conducting MOFs.

Supplementary material

CCDC-988934 contains the supplementary crystallographic data for this article. These data can be obtained free of charge from The Cambridge Crystallographic Data Center via www.ccdc.cam.ac.uk/data_request/cif.

Funding

This work was supported by the National Natural Science Foundation of China [grant number 21171050]; the Program for Innovative Research Team in University of Henan Province [grant number 2012IRTSTHN006]; the Program for Innovative Research Team (in Science and Technology) in University of Henan Province [grant number 13IRTSTHN026].

References

[1] K.D. Kreuer, S.J. Paddison, E. Spohr, M. Schuster. *Chem. Rev.*, **104**, 4637 (2004).
[2] (a) M.L. Wei, Y.X. Wang, X.J. Wang. *J. Solid State Chem.*, **209**, 29 (2014); (b) M.L. Wei, J.H. Wang, Y.X. Wang. *J. Solid State Chem.*, **108**, 323 (2013).
[3] (a) M.L. Wei, X.X. Wang, X.Y. Duan. *Chem. Eur. J.*, **19**, 1607 (2013); (b) M.L. Wei, X.X. Wang, J.J. Sun, X.Y. Duan. *J. Solid State Chem.*, **202**, 200 (2013).
[4] (a) N.C. Jeong, B. Samanta, C.Y. Lee, O.K. Farha, J.T. Hupp. *J. Am. Chem. Soc.*, **134**, 51 (2012); (b) M. Sadakiyo, H. Okawa, A. Shigematsu, M. Ohba, T. Yamada, H. Kitagawa. *J. Am. Chem. Soc.*, **134**, 5472 (2012); (c) C. Dey, T. Kundu, R. Banerjee. *Chem. Commun.*, **48**, 266 (2012).
[5] (a) M.L. Wei, C. He, Q.Z. Sun, Q.J. Meng, C.Y. Duan. *Inorg. Chem.*, **46**, 5957 (2007); (b) M.L. Wei, C. He, W.J. Hua, C.Y. Duan, S.H. Li, Q.J. Meng. *J. Am. Chem. Soc.*, **128**, 13318 (2006); (c) C.Y. Duan, M.L. Wei, D. Guo, C. He, Q.J. Meng. *J. Am. Chem. Soc.*, **132**, 3321 (2010).
[6] SMART and SAINT. *Area Detector Control and Integration Software*, Siemens Analytical X-ray Systems Inc., Madison, WI (1996).
[7] G.M. Sheldrick. *(SHELXTL Version 5.1), Software Reference Manual*, Bruker AXS, Inc., Madison, WI (1997).
[8] (a) M.L. Wei, H.Y. Xu, R.P. Sun. *J. Coord. Chem.*, **62**, 1989 (2009); (b) M.L. Wei, R.P. Sun, K. Jiang, L. Yang. *J. Coord. Chem.*, **61**, 3800 (2008); (c) M.L. Wei, P.F. Zhuang, H.H. Li, Y.H. Yang. *Eur. J. Inorg. Chem.*, **2011**, 1473 (2011); (d) M.L. Wei, P.F. Zhuang, Q.X. Miao, Y. Wang. *J. Solid State Chem.*, **184**, 1472 (2011); (e) M.L. Wei, P.F. Zhuang, J.H. Wang, X.X. Wang. *J. Mol. Struct.*, **995**, 51 (2011); (f) C.J. Zhang, H.J. Pang, D.P. Wang, Y.G. Chen. *J. Coord. Chem.*, **63**, 568 (2010); (g) Y.Z. Fu. *J. Coord. Chem.*, **63**, 1856 (2010); (h) M.L. Wei, H.H. Li, G.J. He. *J. Coord. Chem.*, **64**, 4318 (2011); (i) Q. Deng, C.L. Zhang, J.T. Tang, S.Z. Lu, H.L. Ma, T.J. Cai. *J. Coord. Chem.*, **65**, 3458 (2012); (j) J.Y. Guo, X.F. Jin, L. Chen, Z.X. Wang, Y. Xu. *J. Coord. Chem.*, **65**, 3821 (2012); (k) J. Li, Y. Huang, Q.X. Han. *J. Coord. Chem.*, **66**, 2405 (2013); (l) L.M. Wang, H.Y. Guo, S. Li, Y.Y. Hu, Y. Wang, L.N. Xiao, D.C. Zhao, Z.M. Gao, D.F. Zheng, X.B. Cui, Y. Fan, J.Q. Xu. *J. Coord. Chem.*, **67**, 728 (2014).
[9] (a) S. Bureekaew, S. Horike, M. Higuchi, M. Mizuno, T. Kawamura, D. Tanaka, N. Yanai, S. Kitagawa. *Nat. Mater.*, **8**, 831 (2009); (b) A. Shigematsu, T. Yamada, H. Kitagawa. *J. Am. Chem. Soc.*, **133**, 2034 (2011); (c) N.C. Jeong, B. Samanta, C.Y. Lee, O.K. Farha, J.T. Hupp. *J. Am. Chem. Soc.*, **134**, 51 (2012); (d) M. Sadakiyo, T. Yamada, H. Kitagawa. *J. Am. Chem. Soc.*, **131**, 9906 (2009); (e) J.M. Taylor, R.K. Mah, I.L. Moudrakovski, C.I. Ratcliffe, R. Vaidhyanathan, G.K.H. Shimizu. *J. Am. Chem. Soc.*, **132**, 14055 (2010); (f) C. Dey, T. Kundu, R. Banerjee. *Chem. Commun.*, **48**, 266 (2012); (g) S. Ohkoshi, K. Nakagawa, K. Tomono, K. Imoto, Y. Tsunobuchi, H. Tokoro. *J. Am. Chem. Soc.*, **132**, 6620 (2010).
[10] K.D. Kreuer, A. Rabenau, W. Weppner. *Angew. Chem. Int. Ed.*, **21**, 208 (1982).